JOURNAL OF THERMOPHYSICS AND HEAT TRANSFER
Vol. 21, No. 2, April–June 2007

Theoretical Predictions of Hydrogen Recombination on Zirconia

F. Finamore* and C. Bruno†
University of Rome "La Sapienza," 00184 Rome, Italy

DOI: 10.2514/1.15322

A model of catalytic recombination of hydrogen over zirconia is reported. Zirconia is the main thermal barrier coating in many propulsion systems, and has been proposed also for nozzle facility to test Rubbia's nuclear engine using hydrogen propellant. Because hydrogen temperature may reach 6000 K, part of the heat load may be due to catalytic recombination of H atoms over zirconia. The structural features of zirconia lend themselves to derive a kinetic model similar to that already proposed by Bruno for O and N recombination over silica. This model is applied to conditions representative of high temperature hydrogen expanding in a zirconia-coated nozzle. The range of recombination probability is calculated as a function of model parameters. The heat load is calculated accounting for chemical energy accommodation that is chosen by estimating the most efficient recombination mechanism. The results show that the chemical energy accommodation $\sim 8 \times 10^{-5}$ and that the heat flux at the nozzle throat due to heterogeneous recombination of hydrogen is of order $\mathcal{O}(10^{-1})$ MW/m^2 for surface temperature of the order of 1000 K. The kinetic model proposed is therefore capable of preliminary predictions of heterogeneous recombination, if the surface crystal structure is known, narrowing experimental matrices and reducing testing cost.

Nomenclature

ads	=	adsorption
A_e	=	nozzle exit area
A_t	=	throat cross section area
A_x	=	area of nozzle cross section at station x from throat
B_e	=	rotational constant
c	=	speed of light
d	=	distance from an O atom to the first surface layer
D_e	=	diatom bond energy
D_{mi}	=	diffusion coefficient of species i
Da_{Wi}	=	catalytic heterogeneous Damköhler number of species i
E_a	=	adsorption activation energy
E_e	=	electronic energy
E_m	=	migration activation energy
E_r	=	rotational energy
E_T	=	total energy
E_v	=	vibrational energy
H°	=	enthalpy of formation
h	=	Planck constant
I_{sp}	=	specific impulse
K	=	thermal conductivity
K_{Wi}	=	surface catalytic recombination rate (catalyticity) of the species i
k	=	Boltzmann constant
m_A	=	atomic mass
m_i	=	mass of species i
m_M	=	molecular mass
N	=	number of sites per unit area
N_{coll}	=	number of collisions between adatoms per unit time and unit area
N_m	=	number of recombined molecules per unit time and unit area
n	=	molar fraction
P_{ER}	=	Eley–Rideal steric factor
P_m	=	molecular steric factor
p_A	=	partial pressure of atoms
p_M	=	partial pressure of molecules
Q_a	=	adsorption energy (bond energy between adatom and surface)
Q_{ER}	=	Eley–Rideal activation energy
Q_{LH}	=	Langmuir–Hinshelwood activation energy
Q_{lh}	=	energy jump in recombining two adsorbed atoms to form a gas molecule
$\dot{q}$	=	flux of energy actually entering the catalyst surface
R	=	molar gas constant
r	=	distance between two atoms
r_e	=	equilibrium distance between two atoms (bond distance of a diatomic molecule)
s	=	sticking coefficient
s_a	=	initial atomic sticking coefficient (all the sites empty)
s_m	=	initial molecular sticking coefficient (all the sites empty)
T	=	temperature
T_f	=	melting temperature
T_W	=	wall temperature
V	=	atomic potential (due to crystal atoms)
v_{A^*}	=	mobile adatom velocity (mean velocity of adatoms assuming a two-dimensional kinetic theory gas)
Z_A	=	flux of impinging atoms
$Z_{A,aA}$	=	flux of adsorbed atoms
$Z_{A,ads}$	=	total flux of adsorbed atoms
$Z_{A,aM}$	=	flux of adsorbed molecules
$Z_{A,dER}$	=	flux of molecules recombined by Eley–Rideal mechanism
$Z_{A,des}$	=	total flux of desorbed atoms
$Z_{A,dLH}$	=	flux of molecules recombined by Langmuir–Hinshelwood mechanism
$Z_{A,dTH}$	=	flux of atoms leaving the surface not recombined
$Z_{A,REC}$	=	flux of desorbing adatoms recombined as molecules
Z_M	=	flux of impinging molecules
α	=	thermal dilatation coefficient
β	=	chemical accommodation coefficient
γ	=	recombination probability
γ^*	=	microscopic Rideal-recombination coefficient
Δ	=	minimum distance between two sites
θ	=	coverage coefficient

Received 29 December 2004; accepted for publication 23 October 2005.

*Researcher, Department of Mechanics and Aeronautics, Via Eudossiana 18.

†Professor, Department of Mechanics and Aeronautics, Via Eudossiana 18. Associate Fellow AIAA.

μ = reduced mass
ν = number of sites reached by a moving adatom per unit time
τ_{dif} = diffusion characteristic time
τ_{hc} = heterogeneous chemistry characteristic time
ω = spectral frequency
ω_e = vibrational constant

I. Introduction

THE original motivation for this work was the need to estimate heat deposition due to hydrogen atoms recombination inside the nozzle for the test facility planned by the Italian Space Agency for the Project 242, assessing in this way the feasibility of a nuclear rocket engine based on heating hydrogen gas by means of thin-layer fission of a transuranic isotope (^{242m}Am) [1]. Approximately half of its fission fragments thermalize inside the hydrogen propellant, raising its temperature to 6000–8000 K and dissociating it. Nozzle expansion may result in generating specific impulse in the range 1800–2500 s provided heat transfer inside the stagnation chamber and along the nozzle may be adequately controlled. The future engine will consist of a cluster of modular stagnation chambers; accordingly, the text facility will test a single chamber connected to a nozzle. With respect to a full-size engine: near the throat the heat flux is therefore larger $\sim$50 MW/m^2, [2], and about the same as in (disposable) solid rocket motors. In [2] the heat flux was estimated assuming a zirconia-coated tungsten nozzle. The cooling strategy proposed [2,3] consists of circulating liquid Na in an annular nozzle jacket. In this context, but also for other applications where H atoms are a significant species (e.g., in plasma torches), it is important to establish zirconia (ZrO_2) catalyticity and its associated thermal flux.

To this purpose a model is presented here for catalytic recombination of H over ZrO_2 that follows the approach developed in [4] for O and N over silica. Although the model is still crude, it may be useful as a preliminary design tool to reduce as much as possible expensive testing.

II. Zirconia Features

Tungsten is assumed as the nozzle structural material because its high melting point ($T_f = 3137$ K) reducing enthalpy losses to the wall. However, tungsten cannot be in direct contact with hydrogen because of its reactivity [2] (hot corrosion) and must be coated. Among thermal barrier coating (TBC), zirconia has high T_f (2900 K), low reactivity, and a thermal dilatation coefficient, $\alpha = 5.6 \times 10^{-6\circ}\text{C}^{-1}$, very close to that of tungsten ($4.98\times 10^{-6\circ}\text{C}^{-1}$).

Zirconia exists in three stable phases (cubic, tetragonal, monocline) in three temperature ranges (2727–2370°C, 2370–1170°C, 1170°C ambient temperature, respectively); volumetric changes during phase transitions may cause cracks. Adding more than 8% of oxides such as Y_2O_3, CaO, or MgO to ZrO_2 stabilizes its cubic phase in the entire range of temperatures of interests. However, to prevent cracks Partially Stabilized zirconia, PSZ, (oxide fractions <8%) is preferable because of its slight volume changes with temperature.

The thermal conductivity of ZrO_2 is 0.77–1.11 W/mK, compared with that of tungsten, 118 W/mK: this is the main reason for using ZrO_2 as a TBC.

Hydrogen reacts much less with zirconia than with tungsten; however, both 2-D nonequilibrium and 1-D equilibrium simulations using the NASA CEA Code 400 predict a molar concentration of H $\sim$99% at the throat and $\sim$60% at the nozzle exit. Such calculations suggest H recombination on the colder zirconia walls is possible. The $H + H \rightarrow H_2$ recombination is strongly exothermic ($D_{e\text{H2}} =$ 436 kJ/mol) [5], therefore catalysis could substantially add to the conduction heat load to the wall, with similar impact on the nozzle cooling system. For this reason even crudely estimating the catalytic efficiency of ZrO_2 on H + H recombination is necessary.

III. Heterogeneous Catalysis Model

The heterogeneous catalysis model is patterned after that in [4]. This model strives to account for all the relevant elementary processes involved; its goal is to find, the recombination probability γ defined as

$$\gamma = \frac{\text{flux of atoms recombining at suface}}{\text{flux of atoms impringing at suface}} \tag{1}$$

The flux of impinging atoms/molecules is determined in these models from the kinetic theory of gases: for example, the flux of impinging atoms over a planar surface is

$$Z_{A,M} = p_{A,M}/\sqrt{2\pi m_{A,M} kT} \tag{2}$$

The recombination reaction mechanism is assumed to consist of four steps: diffusion to the surface, adsorption, surface chemical reactions, and desorption from the surface. These steps are modeled yielding eventually the recombination coefficient γ. A short description of these steps follows.

Adsorption may be the following: associative, typical of individual atoms; and dissociative, exemplified by the breaking of molecular bonds of diatomic molecules.

The fraction of impinging particles adsorbed is proportional to s representing the adsorption probability: $Z_{\text{adsorbed particles}} = sZ_{\text{impinging particles}}$. The coefficient s depends mainly on probability to strike a free site. The coverage coefficient θ defined as $\theta =$ (number of filled sites/number of sites) is a measure of the probability that a site is occupied by an atom.

In the case of gas atoms, adsorption is assumed not activated; however, its probability is not unity, because the impact angle might not allow it, or the energy of a striking atom could be so high as to prevent it from staying on the surface long enough to be adsorbed: s_a accounts for these and other effects. In the case of molecules, adsorption is modeled as to depend on an E_a, and P_m accounting for the trajectory of the molecule impacting the surface.

Based on these considerations, the flux of adsorbed atoms is

$$Z_{A,aA} = s_a(1-\theta)Z_A \tag{3}$$

and that of adsorbed molecules

$$Z_{A,aM} = 2(1-\theta)^2 \underbrace{P_m e^{-E_a/RT} Z_M}_{s_m} \tag{4}$$

Following adsorption, atoms recombine to molecules through an Eley–Rideal reaction, E–R, where flux of atoms recombined with this mechanism is

$$Z_{A,d\text{ER}} = \theta Z_A P_{\text{ER}} e^{-Q_{\text{ER}}/RT} \tag{5}$$

with P_{ER} accounts for impact orientation and other unknowns, and a Langmuir–Hinshelwood reaction, L–H, when two adatoms have sufficient energy to move on the surface, collide, and react. Its flux of recombined atoms is

$$Z_{A,d\text{LH}} = 2Nm = \nu N\theta^2 e^{-Q_{\text{LH}}/RT} \tag{6}$$

N_m depends on N_{coll} (per unit time and area)

$$\text{N}_{\text{coll}} = \frac{1}{2}\underbrace{\frac{v_{A^*}}{\Delta}}_{\nu} \underbrace{\text{N}\theta^2 e^{-Em/RT}}_{\substack{\text{number of}\\ \text{mobile adatoms}}} \tag{7}$$

$$\text{N}_m = N_{\text{coll}} e^{Q_{LH}/RT} \tag{8}$$

Because adatoms must have energy greater than E_m to move on the surface, the frequency of collisions ν in Eq. (7) is assumed as the ratio between v_{A^*}, and Δ. For a two-dimensional gas the velocity v_{A^*} is

$$v_{A^*} = \sqrt{\pi kT/(2m_A)} \tag{9}$$

In Eq. (8), the activation energy Q_{LH} is the larger between E_m and Q_{lh}.

Following E–R or L–H recombination, the molecule can desorb. Adatoms with sufficient energy can leave the surface without recombining (thermal desorption). Its flux is

$$Z_{A,d\mathrm{TH}} = N\theta(kT/h)e^{-Qa/RT} \tag{10}$$

The total flux of adatoms desorbing as recombined molecules is therefore

$$Z_{A,\mathrm{REC}} = Z_{A,Aa} - Z_{A,d\mathrm{TH}} + Z_{A,d\mathrm{ER}} \tag{11}$$

and because

$$Z_{A,\mathrm{REC}} = \gamma(Z_A + 2Z_M) \tag{12}$$

equating Eqs. (11) and (12), together with the flux expressions, Eqs. (3), (5), and (10), yields the γ sought

$$\gamma = s_a(1-\theta) - (NkT/Z_A h)e^{-Qa/RT}\theta + \gamma^*\theta \tag{13}$$

In Eq. (13), the factor γ^* represents the probability of a successful formation of the molecule when an atom from the gas strikes an adatom, and it is possible to express as

$$\gamma^* = P_{\mathrm{ER}}e^{-Q_{\mathrm{ER}}/RT} \tag{14}$$

The coverage coefficient θ in Eq. (13) is calculated assuming a steady-state dynamical equilibrium, between adsorption and desorption:

$$Z_{A,\mathrm{ads}} = Z_{A,\mathrm{des}} \rightarrow Z_{A,aA} + Z_{A,aM} = Z_{A,d\mathrm{LH}} + Z_{A,d\mathrm{ER}} + Z_{A,d\mathrm{TH}} \tag{15}$$

Substituting the expression of the fluxes with Eqs. (3–6) and (10) on the right and left term of Eq. (15), the equation for θ to solve together with Eq. (13) is

$$s_a(1-\theta) + 2(Z_M/Z_A)s_m(1-\theta)^2 = \gamma^*\theta + (\nu \mathrm{N}/Z_A)e^{-Q_{\mathrm{LH}}/RT}\theta^2 + (NkT/Z_A h)^{-Qa/RT}\theta \tag{16}$$

IV. Estimating Catalytic Model Parameters

Predictions using Eqs. (13) and (16) require knowledge of several energy parameters. The interaction forces between zirconia and hydrogen depend on the crystal structure of zirconia. The layers of crystal atoms most influential on an adatom are assumed as "the surface." To simplify the problem, zirconia is assumed pure; this assumption is only fair, because the percentage of mixed oxides is less 8%. The crystal structure of zirconia is a face-centered cube of zirconium atoms, enclosing a cube of oxygen atoms. To apply the catalytic model, the crystal plane that interacts with gas must be determined.

When a crystal interacts with a gas, crystal atoms are displaced, tending toward the minimum free energy lattice configuration. That occurs when the crystal enables the maximum number of significant interactions with the gas, typically when the crystal face with major density of crystal atoms is oriented toward the gas. In zirconia, this face is the Miller plane ⟨111⟩, also most information is available for this face; for this reason plane ⟨111⟩ is assumed as the exposed face (Fig. 1):

The next step is to determine which is the first crystal layer impacted by the gas atoms or molecules. The zirconia surface can be visualized as a layer of zirconium coated by an oxygen cloud that interacts with impinging hydrogen atoms. In fact, the electronic affinity of oxygen for H (141 kJ/mol) is greater than that of zirconium (41.1 kJ/mol): H tends to bind with O rather than with Zr. In fact, FT–IR spectroscopy of H (atomic and molecular) over zirconia shows the existence of Zr–OH spectrum peaks [6,7].

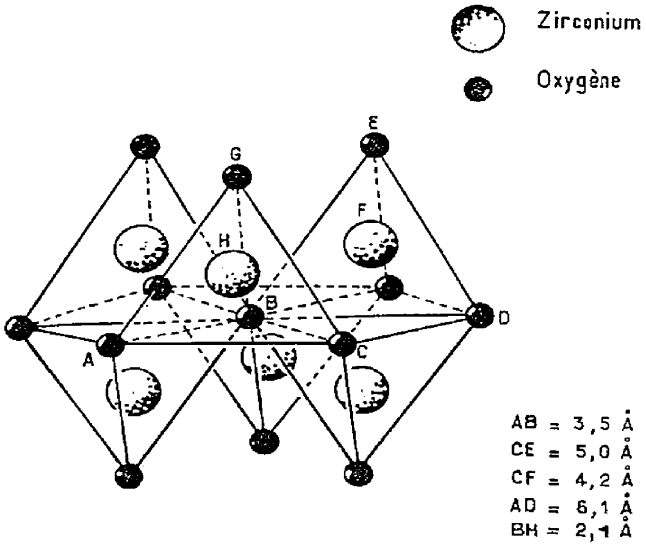

Fig. 1 Miller plane ⟨111⟩ of the ZrO_2 crystal [28].

Catalytic "sites" are defined as locations where H atoms are fully chemiadsorbed (i.e., where the H interaction potential with the surface is lowest). The parameters ($Q_{\mathrm{LH}}, Q_{\mathrm{ER}}, E_m, Q_a, \nu$) in Eqs. (13) and (16) depend on site locations and on the minimum interaction potential among adatom and crystal; both are calculated when the crystal structure and first crystal layer impacted by the gas particles are defined. So the next step is to calculate the interaction potential, V_{H}, of hydrogen with the surface allowing to define energy barriers and sites location.

For a single H (gas) and O (crystal) pair, the site is the location of the crystal oxygen, and the lowest potential would be that of the OH bond energy (427.8 kJ/mol) [8]. However, for a surface the total hydrogen-surface potential must be calculated by adding the contributions of the most influential crystal atoms along the surface and in the sublayers.

The potential assumed here is the Morse potential [9] more accurate than a simple harmonic potential.

Taking advantage of its additive property, the hydrogen Morse potential due to the surface, first layer, and more influent sublayers is assumed as the sum of single H (gas)–O (crystal) pairs, thus simplifying the calculations. The Morse potential for a single pair of atoms is

$$V(r) = D_e\{1 - e^{[-\varepsilon(r-r_e)]}\}^2 \tag{17}$$

with:

$$\varepsilon = \frac{1}{2}\omega\left(\frac{2\mu}{D_e}\right)^{\frac{1}{2}} = 2\pi c\omega_e\left(\frac{\mu}{2D_e}\right)^{\frac{1}{2}}\ [\mathrm{m}^{-1}] \tag{18}$$

where r_e is a function of the rotational constant B_e

$$r_e = (h/8\pi^2 cB_e\mu)^{\frac{1}{2}} \tag{19}$$

with μ is the reduced mass $m_{\mathrm{atomA}}m_{\mathrm{atom}B}/m_{\mathrm{atomA}} + m_{\mathrm{atom}B}$. The Morse potential can be calculated when the three parameters B_e, D_e, ω_e can be found for instance from spectral analysis [10].

The Huges expression of the Morse potential is [11]:

$$V(r) = D_e[(1 - e^{-\varepsilon(r-r_e)})^2 - 1] \tag{20}$$

By defining

$$\begin{cases} y = (r - r_e)/r_e = L - 1 \\ L = r/r_e \\ b = \varepsilon r_e \end{cases} \tag{21}$$

the Huges expression of the potential becomes

$$V(r) = D_e[(1 - e^{-\varepsilon(r-r_e)})^2 - 1] \tag{22}$$

So, the potential of a hydrogen adatom due to its surface interaction is

$$V_H(x) = \sum V_{OH} + \sum V_{ZrH} \tag{23}$$

The sum $\sum$ should include all the lattice atoms, however, generally, the first three layers of the surface are the most influential.

The potential of O–H pairs is also affected by zirconium atoms. A review of spectra literature did not find information on the bond energy of ZrO–H; consequently, this parameter is calculated by applying the Hess law. The D_e of ZrO–H is equal to the enthalpy of the reaction $ZrOH(g) = ZrO(g) + H(g)$, also unknown but also a step of the chain:

$$\begin{array}{lcll} ZrOH(g) = Zr(g) + OH(g) & \rightarrow & \Delta H^\circ = 527 \text{ kJ/mol} & \text{Ref. [6]} \\ Zr(g) + O(g) = ZrO(g) & \rightarrow & \Delta H^\circ = -764.6 \text{ kJ/mol} & \text{Ref. [8]} \\ OH(g) = O(g) + H(g) & \rightarrow & \Delta H^\circ = 427.8 \text{ kJ/mol} & \text{Ref. [8]} \end{array}$$

$$\text{therefore } ZrOH(g) = ZrO(g) + H(g) \quad \rightarrow \quad \Delta H^\circ = 190.2 \text{ kJ/mol}$$

The D_e of ZrO–H calculated as $D_{e(\text{O–H})} = 190.2$ kJ/mol implies the zirconium atom weakens the O–H bond that, without Zr, would be 427.8 kJ/mol [8].

The other parameters sought are $r_{e(\text{O–H})} = 0.96$ *BROKEN*, from [5], B_e, calculated using Eq. (19), and $\omega_{e(\text{O–H})}$. Spectral data [7,12,13] for hydroxyls on zirconia report different values of ω for O–H. The value $\omega_{e(\text{O–H})} = 3660$ cm^{-1} [14] was preferred because experimental conditions (ZrO_2–Y_2O_3 and a Miller plane $\langle 111 \rangle$) were the closest to those of this study.

The spectral literature on Zr–H is broad but often not self-consistent. The parameters $r_{e(\text{Zr–H})}$ and $\omega_{e(\text{Zr–H})}$ were taken from [15], where $r_{e(\text{Zr–H})} = 1.77$ *BROKEN* and $\omega_{e(\text{Zr–H})} = 1777$ cm^{-1}. Data of [15] were preferred to those in [16,17], because estimated $D_{e(\text{Zr–H})}$ is close to that calculated using thermodynamics, and also because the other two parameters ($r_{e(\text{Zr–H})}, \omega_{e(\text{Zr–H})}$) are near the average of values estimated by other spectral studies. Applying again the Hess law:

$$\begin{array}{lcll} Zr(s) + \frac{1}{2}H_2(g) = ZrH(g) & \rightarrow & \Delta H^\circ = 517.346 \text{ kJ/mol} & \text{Ref. [8]} \\ Zr(g) = Zr(s) & \rightarrow & \Delta H^\circ = -602.1 \text{ kJ/mol} & \text{Ref. [8]} \\ H(g) = \frac{1}{2}H_2(g) & \rightarrow & \Delta H^\circ = -216.035 \text{ kJ/mol} & \text{Ref. [8]} \end{array}$$

$$Zr(g) + H(g) = ZrH(g) \qquad \Delta H^\circ = -300.8 \text{ kJ/mol}$$

So, the enthalpy of reaction $ZrH(g) = Zr(g) + H(g)$ is assumed equal to Zr–H bond energy, and therefore $D_{e(\text{Zr–H})} = 300.8$ kJ/mol.

The potential functions V_{ZrH} and V_{OH} in Eq. (24) are then written by substituting the two sets of parameters (r_e, D_e, ω_e) just found inside Eqs. (18), (19), (22), and (23). Which surface atoms affect V_{H} is estimated by comparing the V_{ZrH} and V_{OH} calculated for several O–H and Zr–H pairs along the same layer and varying the layer. In summary, the configuration of the most influential atoms is found to depend on three surface layers, as sketched in Fig. 2:

This configuration is assumed as the elementary cell to calculate V_{H}, adding the contribution of all three layers. The minimum of $V_{\text{H}}(x)$ (-391.424 kJ/mol, at $r_e = 0.93$ *BROKEN*) corresponds to a likely adsorption site.

Accounting for the effect of other crystal atoms (Zr and O), beside of single O (surface)–H (adatom) pairs, strengthens the H-surface bond, with respect to the single O–H pair (391.424 kJ/mol vs 190.2 kJ/mol), as the bond distance decreases from 0.96 to 0.93 Å. However, this energy might not be equal to the adsorption energy Q_a, sought. Adsorption occurs in the deepest potential well; the $V_{\text{H}_{\min}}$ just calculated is only a local minimum for the configuration of Fig. 2. Local minima $V_{\text{H}_{\min}}$ must be calculated at every surface location of H, the lowest corresponding to the H adsorption state.

We assume that the lowest $V_{\text{H}_{\min}}$ lies on line between two adjacent oxygen atoms on the first layer (they are the closest to H). Looking at Fig. 2, successive $V_{\text{H}_{\min}}$ were calculated by moving H along the shortest path between two O atoms on the first layer. Besides the point 1 just evaluated other significant locations are point 2, at $r_e = 0.93$ *BROKEN* from the nearest O, and point 3, in the middle of the O–O path, at the distance 1.75 Å from both nearest O atoms. At both these points the most influential crystal atoms are found by adding other elementary cells to that shown in Fig. 2; which Zr and O of the cluster influence more V_{H} is determined by comparing V_{OH} and V_{ZrH}. For instance, at point 3 ($d = 1.75$ *BROKEN*), there are 14 influential atoms situated on different cells, whereas at point 1 they are 13 and located only in the elementary cell of Fig. 2. V_{H} is calculated by applying Eqs. (22) and (24) to the most influential atoms found at point 2 and point 3. The $V_{\text{H}_{\min}}$ turn out to be -259.865 kJ/mol at point 2, and -483.209 kJ/mol at point 3. The conclusion is that this last is the deepest potential well and that the sites are located in the middle of the line joining two adjacent O atoms located on the first layer, with adsorption energy $Q_a = -V_{\text{H}_{\min 3}} = 483.209$ kJ/mol. The $V_{\text{H}_{\min}}$ function along d is shown in Fig. 3.

$V_{\text{H}_{\min}}$ allows to estimate the sites location and therefore the minimum distance between two sites, $\Delta = 1.75$ *BROKEN*, hence the density of sites, $N = 6.28 \times 10^{18}$ m^{-2}.

In fact, adsorption can occur at any minimum of the potential energy surface where the well depth is comparable to the typical interaction energy assumed for chemisorption, increasing N with respect the density just calculated. These other sites, where there is not deepest potential well, should not affect significantly catalytic heat flux, because their residence time is low, however, an improvement of our model will take into account also these other sites.

The migration energy E_m, equal to the difference between the adsorption energy and the maximum $V_{\text{H}_{\min}}$, is found to be $E_m = 223.344$ kJ/mol.

V. Application of the Model to the Hydrogen/Zirconia Case

Some of the assumptions in the [3] will be kept and others will be relaxed in applying the model just presented to H/ZrO_2 recombination. Assume, for the time being only, that there is complete chemical energy accommodation (CEA), $\beta = 1$. The literature on similar cases (e.g., O/O_2 on SiO_2, [18]) points out that $\beta = 1$ is reasonable only for the L–H mechanism, whereas for tin E–R recombination $\beta \ll 1$. The $\beta = 1$ assumption will be dealt in with more detail later. It is also assumed that the nozzle cooling system maintains surface temperature uniform,

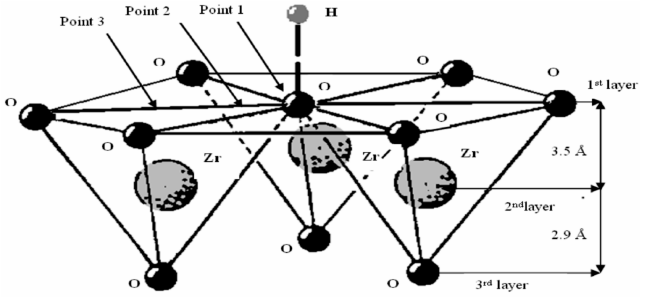

Fig. 2 Configuration of the most influential atoms shaping V_H (elementary cell).

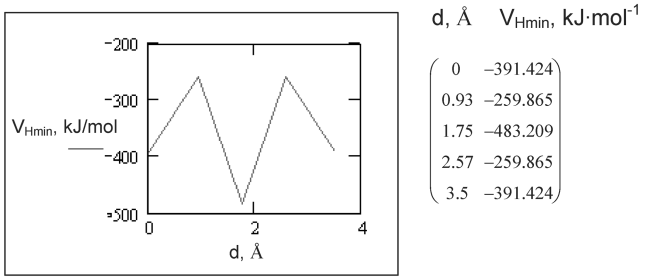

d, Å V_{Hmin}, kJ·mol^{-1}

0	−391.424
0.93	−259.865
1.75	−483.209
2.57	−259.865
3.5	−391.424

Fig. 3 $V_{H_{min}}$ vs distance between two adjacent Oxygen atoms on the first layer.

$T_{wall} = 1000$ K. The flux in the nozzle is assumed isentropic, in thermochemical equilibrium and chocked at the throat. The latter assumptions are reasonable, simplify analysis of model predictions, and can be relaxed without prejudice to the model.

To determine γ the Q_{ER} and Q_{LH} in the adsorption and desorption fluxes must be calculated using the result just found.

The flux of adsorbed H modeled by Eqs. (2) and (4) depends on s_a, a parameter not found in the literature. The flux of adsorbed H_2 is from Eqs. (3) and (5). Dissociative adsorption of H_2 may occur, because the minimum distance between two zirconia sites ($\Delta = 1.75$ *BROKEN*) is close to the diameter of H_2 (1.48 *BROKEN*, in the ground state [5]). Dissociative adsorption is not activated; the energy barrier E_a is negative

$$E_a = \Delta E = V[\mathrm{H\,(ads)} + \mathrm{H\,(ads)}] - V[\mathrm{H_2\,(gas)}] \qquad (24)$$

because $V[\mathrm{H\,(ads)}] = -Q_a = -483.209$ kJ/mol, $V[\mathrm{H_2\,(gas)}] = -D_{eH2} = -436$ kJ/mol.

Assuming $E_a = 0$ in Eq. (5), P_m is equal to s_m; again, there are no literature data on s_m and P_m for H_2 adsorption on ZrO_2. So, P_m (or s_m) and s_a are missing parameters in modeling adsorption fluxes. These fluxes depend also on the p_H and p_{H_2} pressures at the wall requiring complete knowledge of the nozzle gas dynamic field. If it is reasonable to assume the pressure roughly uniform on the nozzle cross section, then $p(x)_{wall} = p(x)_{axis}$. The quantities $[p(x)_{axis}, n_i(x)_{axis}, T(x)_{axis}]$ are calculated using the 1-D NASA CEA400 code, from the nozzle geometry (entrance diameter = 40 cm, throat diameter = 0.977 cm, $A_e/A_t = 476$) and the stagnation conditions ($p_i = 6$ atm, $T_i = 9500$ K) [19]. The solution shows that molar fraction n_H decreases along x while n_{H_2} increases, with n_H always $\gg n_{H_2}$. On the wall molar fractions depend on the ratio between diffusion time to the wall and recombination time of $H + H + M \rightarrow H_2 + M$. Short of solving for the complete 3-D Navier–Stokes equations describing this nozzle flow, two extreme cases are chosen to bracket the solution: equilibrium, and frozen flow. Wall and axis molar fractions are equal in the frozen case, whereas for equilibrium the NASA CEA400 code predictions show that the wall molar fraction of H_2 is almost one. The partial pressures at the wall are calculated for these two extreme cases and so is adsorption.

To calculate the flux of particles released by recombination (E–R and L–H) and by thermal desorption, the unknown parameters are: Q_{ER}, Q_{LH}, thermal desorption energy, P_{ER} and s_a.

The E–R mechanism is frequently a nonactivated process: in many cases the bond energy of the recombined molecule is greater than that of the adatom. However, in the case of H on zirconia the bond energies are $D_{eH_2(gas)} = 436$ kJ/mol $< D_{eH(ad-atom)} = 483.209$ kJ/mol.

$$Q_{ER} = \Delta E = V[\mathrm{H_2\,(gas)}] - V[\mathrm{H\,(adatom)}] = -436 - (-483.209) \qquad (25)$$

must be surmounted to activate E–R recombination. In fact, 47.209 kJ/mol is the highest possible value Q_{ER}: the real E–R recombination barrier could be lower, as E–R recombination may occur even though the adatom is not yet at the bottom of the potential well, or when a fraction of the energy barrier is supplied by wall phonons excited by a previous recombination at the same site. Experimental proof of the uncertainty about Q_{ER} is in [20], where H_2 molecules recombined by the E–R mechanism on tungsten reached a vibrational state incompatible with the Q_{ER} calculated as the simple difference between the potential of gas atoms and adatoms. This result can be explained only if the adatom was not yet at the bottom of the potential well. In this sense Q_{ER} is another missing parameter. Also missing is P_{ER}, needed to determine the flux $Z_{H,dER}$ in Eq. (5).

L–H recombination is instead an activated process; in fact, it occurs only at temperatures higher or much higher than those typical of E–R. The energy barrier Q_{LH} is the larger between E_m and Q_{lh}: $Q_{LH} = 2Q_H - D_{eH_2} = 530.418$ kJ/mol. Equation (7) for the flux $Z_{A,dLH}$ assumes collisions between two mobile adatoms: whether this may occur for H(adatom) on zirconia needs verification. At $T_W = 1000$ K the fraction $N_{ads-free}$ of mobile adatoms, assuming $\theta = 1$, is equal to:

$$N_{H\ ads-free}/N_{H\ ads} = e^{-Em/RT} = 2 \cdot 10^{-12} \qquad (26)$$

Thus the fraction of mobile adatoms is so low that the most probable scenario for L–H recombination is a collision between a mobile and a trapped adatom. Consequently Eq. (7) applied to H on zirconia must be modified by multiplying the right term by two (two mobile H adatoms to cause two collisions); this changes also the right hand side of Eq. (6).

Last, Q_a and N, the parameters to calculate the flux $Z_{H,dTH}$ of atoms due to thermal desorption, Eq. (10), are known.

All the adsorption/desorption fluxes must be substituted in Eqs. (13) and (16) to calculate θ and the probability of recombination γ. Because Q_{ER}, P_M, P_{ER}, s_a are unknown, it is not possible to calculate immediately θ and γ. This lack information can be partly compensated by exploring a suitable range of variation of these parameters, to obtain engineering "margins." Furthermore, as noted, adsorption fluxes are calculated in two extreme cases (frozen flow, equilibrium flow). In conclusion, an "exact" solution of the problem cannot be determined at this time, but the range of γ can.

VI. Analysis of the Dependence of γ on Parameters

Because the catalysis model developed by Bruno *et al.* [4] has never been applied to recombination of H/H_2 on ZrO_2, it is useful to verify whether its results for the nozzle already described are plausible before going any further. For frozen flow at the throat, and fixing arbitrarily the unknown parameters ($P_M = 1$, $P_{ER} = 1$, $s_a = 1$ and $Q_{ER} = Q_{ER\,max} = 47.209$ kJ/mol) yields the γ_H (T) shown in Fig. 4:

The γ_H curve has a typical "S" shape, for example, as in N recombination over tungsten [21]. The S shape is due to the different ranges of temperature where the two recombination mechanisms dominate. As the L–H mechanism has activation energy greater than E–R, at $T \leq 1000$ K the most efficient mechanism is E–R, whereas at "high" temperature $T \geq 1000$ K the most efficient mechanism is L–H, and because in every L–H recombination event two adatoms

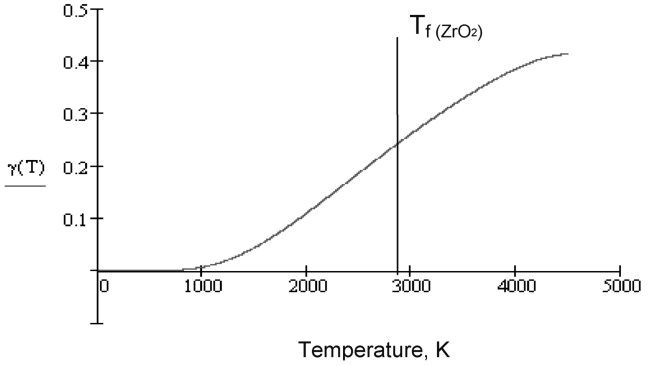

Fig. 4 Predicted hydrogen recombination probability γ_H over zirconia vs temperature at the nozzle throat (frozen flow).

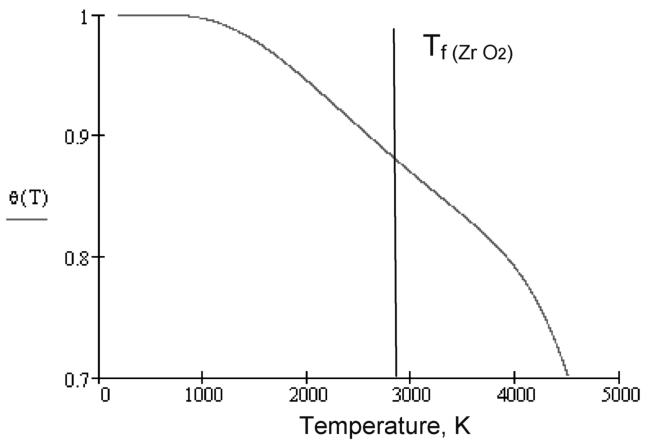

Fig. 5 Coverage coefficient θ over zirconia vs temperature, at the nozzle throat (frozen flow).

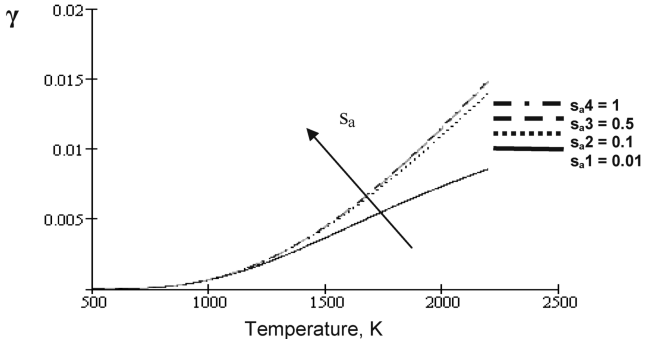

Fig. 6 Dependence of γ_H on the sticking coefficient ($Q_{ER} = 47.209$ kJ/mol, $P_m = 1$, $P_{ER} = 1$).

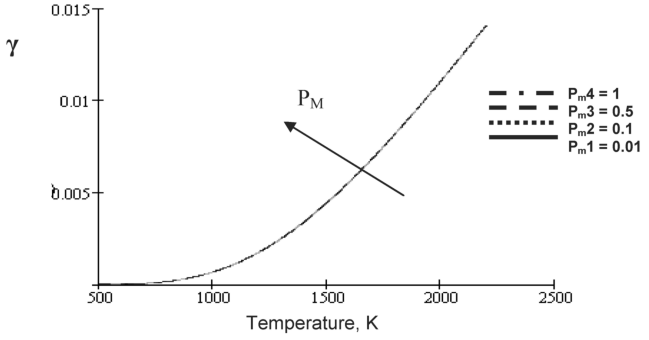

Fig. 7 Dependence of γ_H on the molecular steric factor P_m ($Q_{ER} = 47.209$ kJ/mol, $P_{ER} = 1$, $s_a = 1$).

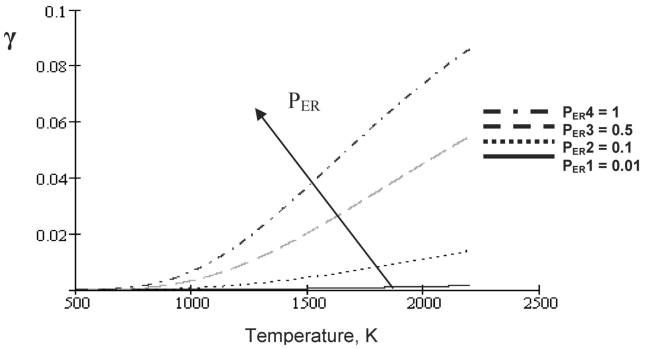

Fig. 8 Dependence of γ_H on the Eley–Rideal steric factor P_{ER} ($Q_{ER} = 47.209$ kJ/mol, $P_m = 1$, $s_a = 1$).

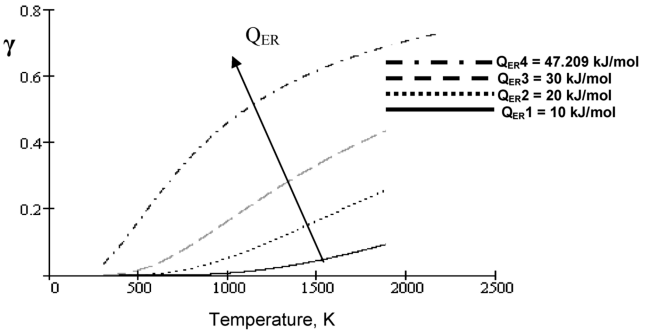

Fig. 9 Dependence of γ_H on the Eley–Rideal activation energy Q_{ER} ($P_m = 1$, $P_{ER} = 1$, $s_a = 1$).

are involved instead of the single atom for E–R, γ_H is correspondingly larger. Figure 4 confirms this typical behavior.

The θ curve calculated for the same conditions (see Fig. 5) is consistent with the $\gamma_H(T)$ trend of Fig. 4, because θ should decrease when the L–H becomes the more efficient mechanism, as for every L–H recombination event two adatoms leave the surface. In fact Fig. 6 shows θ decreasing for $T \geq 1000$ K, the same temperature range were L–H takes over. In essence, Figs. 4 and 5 show the model presented is self-consistent and at least plausible.

Based on this result, the next step is to try to reduce the number of unknown parameters (Q_{ER}, P_m, P_{ER}, s_a). The dependence of γ on one of the unknown parameters is investigated by fixing the remaining three parameters; the throat flow is still assumed frozen. Figures 6–8 show the dependence of γ_H on s_a, P_m, and P_{ER} respectively, assuming $Q_{ER} = 47.209$ kJ/mol. Figure 9 shows the dependence of γ_H on Q_{ER}.

The wall temperature, based also on results in [19], is still 1000 K. Figures 6 and 7 show that at $T = 1000$ K γ_H is only weakly affected by s_a and P_m, suggesting these two parameters are less significant in influencing γ_H, and could be assumed, for instance, unity without prejudicing main results and conclusions. Also such assumption is conservative in designing a nozzle that must withstand heat loads of order $\mathcal{O}(10)$ MW/m^2.

VII. Results and Discussion

The recombination probability γ_H along x is calculated assuming s_a and P_m equal to 1 (the most favorable values for surface recombination), and two extreme gas flow cases (frozen or equilibrium). In both γ_H is calculated by varying Q_{ER} (from 10 kJ/mol to 47.209 kJ/mol) and P_{ER} (from 0.01 to 1). Overall, calculations show that γ_H does not change significantly from the throat to the nozzle exit, see Table 1 (equilibrium case). Table 2 shows that γ_H behaves similarly for the frozen case.

Before commenting the γ results, it is necessary to compare the times of gas diffusion and heterogeneous catalysis times in order to find when the heat flux due to heterogeneous catalysis is dominant. The Damköhler number for catalysis, Da_W [22],

Table 1 γ_H at nozzle throat and at nozzle exit (varying P_{ER}, Q_{ER}). Equilibrium case. $T_W = 1000$ K

Q_{ER}, kJ · mol^{-1}	$P_{ER} = 0.01$		$P_{ER} = 0.5$		$P_{ER} = 1$	
	$A_x/A_t = 1$	$A_x/A_t = 476$	$A_x/A_t = 1$	$A_x/A_t = 476$	$A_x/A_t = 1$	$A_x/A_t = 476$
47.209	3.438×10^{-5}	3.566×10^{-5}	1.712×10^{-3}	1.712×10^{-3}	3.422×10^{-3}	3.422×10^{-3}
30	2.715×10^{-4}	2.752×10^{-4}	0.014	0.014	0.027	0.027
20	9.032×10^{-4}	9.098×10^{-4}	0.045	0.045	0.09	0.09
10	3.005×10^{-3}	3.018×10^{-3}	0.15	0.15	0.3	0.3

Table 2 γ_H at nozzle throat and at nozzle exit (as a function of P_{ER} and Q_{ER}). Frozen case. $T_W = 1000$ K

Q_{ER}, kJ · mol^{-1}	$P_{ER} = 0.01$		$P_{ER} = 0.5$		$P_{ER} = 1$	
	$A_x/A_t = 1$	$A_x/A_t = 476$	$A_x/A_t = 1$	$A_x/A_t = 476$	$A_x/A_t = 1$	$A_x/A_t = 476$
47.209	6.841×10^{-5}	6.841×10^{-5}	3.415×10^{-3}	3.412×10^{-3}	6.818×10^{-3}	6.809×10^{-3}
30	5.419×10^{-4}	5.418×10^{-4}	0.027	0.027	0.053	0.052
20	1.803×10^{-3}	1.802×10^{-3}	0.086	0.085	0.166	0.161
10	5.99×10^{-3}	5.982×10^{-3}	0.261	0.252	0.462	0.443

Table 3 Da_{H_2} at nozzle throat and at nozzle exit (varying P_{ER} and Q_{ER}). Equilibrium case. $T_W = 1000$ K

Q_{ER}, kJ · mol^{-1}	$P_{ER} = 0.01$		$P_{ER} = 0.5$		$P_{ER} = 1$	
	$A_x/A_t = 1$	$A_x/A_t = 476$	$A_x/A_t = 1$	$A_x/A_t = 476$	$A_x/A_t = 1$	$A_x/A_t = 476$
47.209	1.7×10^{-1}	3×10^{-2}	8.5	1.5	1.7×10^{1}	2.9
10	1.5×10^{1}	2.5	7.5×10^{2}	1.2×10^{2}	1.5×10^{3}	2.5×10^{2}

Table 4 Da_H at nozzle throat and at nozzle exit (varying P_{ER} and Q_{ER}). Equilibrium case. $T_W = 1000$ K

Q_{ER}, kJ · mol^{-1}	$P_{ER} = 0.01$		$P_{ER} = 0.5$		$P_{ER} = 1$	
	$A_x/A_t = 1$	$A_x/A_t = 476$	$A_x/A_t = 1$	$A_x/A_t = 476$	$A_x/A_t = 1$	$A_x/A_t = 476$
47.209	3.6×10^{-10}	1.03×10^{-9}	1.8×10^{-8}	4.9×10^{-8}	3.6×10^{-8}	9.9×10^{-8}
10	3.1×10^{-8}	9.1×10^{-8}	1.6×10^{-6}	4.5×10^{-6}	3.1×10^{-6}	9.1×10^{-6}

$$\mathrm{Da}_W = \tau_{\mathrm{dif}}/\tau_{\mathrm{hc}} \tag{27}$$

becomes for the chemical species i:

$$\mathrm{Da}_{Wi} = K_{Wi} Y_i / D_{mi} (\nabla Y_i)_W \tag{28}$$

K_{Wi} is the catalyticity, that can be written, from the Hertz–Knudsen relation [23]

$$K_{Wi} = \gamma \sqrt{kT_W/2\pi m_i} \tag{29}$$

The value of Da_{Wi} characterizes the heterogeneous chemistry-diffusion coupling. When $\mathrm{Da}_{Wi} \gg 1$, the contribute of heterogeneous catalysis to surface heat flux must be accounted for; when $\mathrm{Da}_{Wi} \ll 1$, this contribute is negligible with respect to that of diffusion.

The calculated Damköhler numbers for molecular and atomic hydrogen are shown in the Tables 3 and 4, as a function of two parameters Q_{ER} and P_{ER}:

In the equilibrium case, hydrogen close to the wall is mostly molecular, therefore $\mathrm{Da}_{WH} \ll 1$ is to be expected for the whole range of Q_{ER} and P_{ER}.

As Q_{ER} decreases and P_{ER} increases, Da_{H_2} increases, because the larger γ_H (shown in Table 1) means τ_{hc} is shorter. Catalyticity is substantial ($\mathrm{Da}_{WH_2} \gg 1$) when the activation energy Q_{ER} is low (10 kJ/mol) and $P_{ER} \geq 0.01$; quantitatively, the contribute of catalysis to surface heat flux must be included when $\gamma \approx \mathcal{O}(10^{-1})$.

As shown by Table 1, γ; may be assumed constant along the wall (once Q_{ER} and P_{ER} have been assumed); and any location on the nozzle wall could be used to calculate γ. However, Da_{WH_2} decreases moving from the throat to the nozzle exit, therefore γ at the throat is the parameter of choice to predict the magnitude of catalytic heating.

Figures 10 and 11 show γ_H at the throat, for $T = 1000$ K, $s_a = P_m = 1$, equilibrium or frozen conditions, and for different values of the parameters Q_{ER} (47.209, 30, 20, 10 kJ/mol) and P_{ER} (1, 0.5, 0.01). These plots show that γ_H covers a wide range.

The spread (or rather uncertainty) on γ_H predicted suggests zirconia might be questionable as tungsten coating. If γ_H is actually greater than 0.1 then a considerable increase of heat flux could occur.

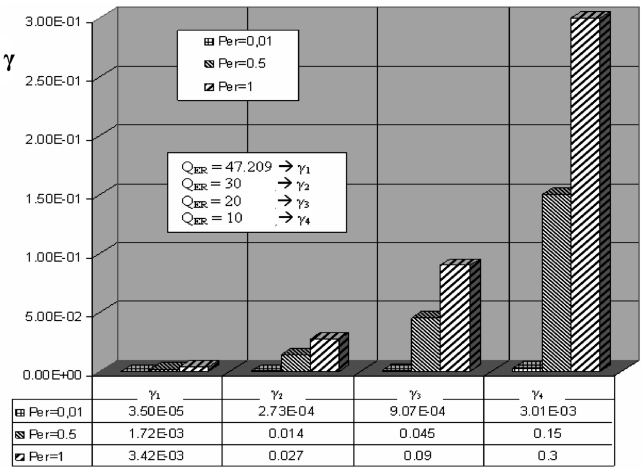

Fig. 10 Dependence of γ on P_{ER} and Q_{ER} (thermochemical equilibrium assumed).

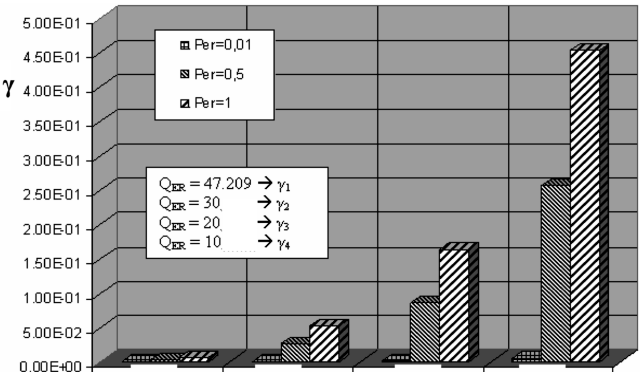

	γ1	γ2	γ3	γ4
Per=0,01	6.84E-05	5.42E-04	1.80E-03	5.99E-03
Per=0,5	3.41E-03	0.027	0.0855	0.2565
Per=1	6.81E-03	0.0525	0.1635	0.4525

Fig. 11 Dependence of γ on P_{ER} and Q_{ER} (frozen flow).

In fact, during shuttle reentry the maximum fraction of heat load due to catalytic recombination is ≈40% [24], the inferred recombination probability being $\gamma \approx 0.01$. Although the gas composition (air) and TBC material (silica) in the shuttle case are different from the ones presented here, it is reasonable to assume a similar match between γ and heat flux also for H on ZrO_2.

VIII. Chemical Energy Accommodation

However, the fraction of the heat load due to surface recombination does not depend only on γ, but also on the CEA coefficient β (see Fig. 12):

The fraction β of recombination energy released to surface is [25]:

$$\beta = \frac{\dot{q}}{D_e Z_{A,\mathrm{REC}}/2} \tag{30}$$

So far, β has been assumed unity: this means $\dot{q}$ is equal to the catalytic heat flux which can be released to the surface. Predictions are difficult because determining $\dot{q}$ would require predicting the energy states of the molecule recombined. Estimating β is easier which recombination mechanism dominate is known. The fraction β depends on the residence time of recombined molecule on the surface. For the L–H recombination this residence time is longer than in the case of E–R recombination [20,25–27], consequently it seems plausible to assume $\beta_{\mathrm{LH}} \approx 1$ and $\beta_{\mathrm{ER}} < 1$. The θ trend depends likewise on the recombination mechanism. When the most efficient recombination mechanism is E–R only one adatom leaves the surface for every recombination event, therefore $\theta \sim 1$, decreasing slowly as T increases. When the most efficient recombination mechanism is L–H, two adatoms leave the surface for every recombination event, and so $\theta < 1$, decreasing rapidly as T increases. The trend of θ is calculated in the present nozzle case assuming $P_m = s_a = P_{\mathrm{ER}} = 1$, varying Q_{ER} in the range already tested, and in the two cases of equilibrium and frozen kinetics. The results are shown in Figs. 13 and 14:

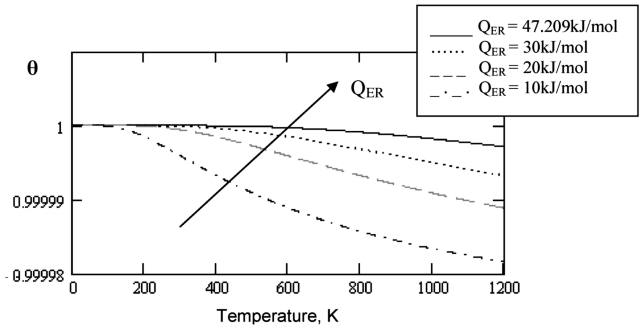

Fig. 13 θ vs temperature (equilibrium case).

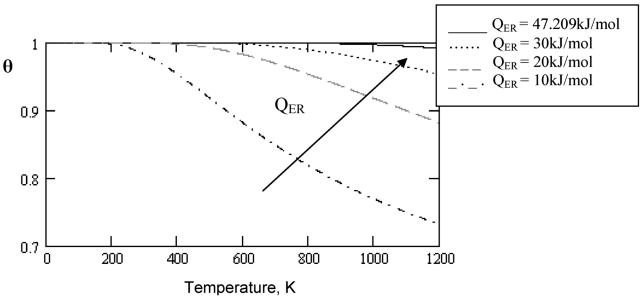

Fig. 14 θ vs temperature (frozen case).

Whether equilibrium or frozen, at $T = 1000$ K, θ is almost equal to 1, implying E–R is the main recombination mechanism and consequently $\beta < 1$. The low β means that also in the worst case ($\gamma = 0.45$) a significant fraction of recombination heat is trapped in the desorbing molecule and not released to the surface.

The catalytic heat flux $\dot{q}$ released to the surface in the case of highest recombination coefficient ($\gamma = 0.45$) can be quantified only if β is known. Because at $T_W = 1000$ K the main mechanism is E–R, approximating β with $\beta_{\min}$ [25] is reasonable, where $\beta_{\min}$ is

$$\beta_{\min} = \frac{Q_a(1-\theta)}{\gamma D_e/2} \tag{31}$$

At $T = 1000$ K, and $\gamma = 0.45$ (case of flow in thermochemical equilibrium, $Q_{\mathrm{ER}} = 10$ KJ/mol and $P_{\mathrm{ER}} = 1$), the coverage θ is ≈0.999; applying Eq. (30) the β predicted, $\beta \sim 8 \times 10^{-5}$, is very low. So, although the maximum γ is high (almost half of the impinging particles recombine), the actual fraction of energy deposited on the surface is negligible. The throat heat flux due to catalysis is then calculated [applying the Eq. (30)] as

$$\dot{q} = \beta_{\min}\left(\frac{Z_{A,\mathrm{REC}} D_{e\mathrm{H}_2}}{2}\right) \tag{32}$$

and is ∼0.42 MW/m^2. In [2], the wall thermal load at throat due to diffusion and conduction was calculated ∼50 MW/m^2: surface catalysis contributes to the wall heat flux at the throat for ∼1% of diffusion and conduction.

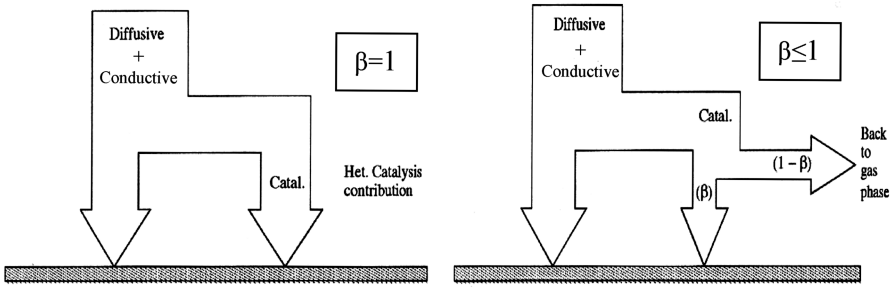

Fig. 12 Distribution of catalytic recombination heat flux between gas and surface.

IX. Conclusions

Because zirconia has been proposed as TBC in the nozzle of the Rubbia's engine, analysis of its catalytic recombination effects on H atoms has been performed.

To this purpose, the total surface heat load has been estimated by developing a heterogeneous catalysis model based on [4]. The zirconia structure has been characterized in a simple way and the interactions between H and surface atoms have been studied and modeled by attempting reasonable estimates of the appropriate energy barriers. This model has been validated by comparing the γ, and θ trend with temperature with those known. The influence of missing parameters (Q_{ER}, P_m, P_{ER}, s_a) on γ has been studied, showing that, at wall $T = 1000$ K, γ_{H} is weakly affected by s_a and P_m. The recombination probability has been calculated by varying Q_{ER} and P_{ER} and for two extreme kinetics cases (frozen or equilibrium). Diffusion and heterogeneous chemistry characteristic times have been compared with find when the heat flux due to heterogeneous catalysis is dominant: results indicate catalysis contributes significantly only when $\gamma \sim \mathcal{O}(10^{-1})$.

At the nozzle throat, the most critical location for heat transfer, catalytic recombination is found high ($\sim$50%) and due mainly to the E–R mechanism. However, most of the catalytic recombination heat is trapped in desorbing molecule ($\beta \ll 1$). Thus, for the conditions examined, the contribution of heterogeneous catalysis to the wall heat flux are predicted very low compared with those due to diffusion and conduction.

As a secondary result of this work, the capabilities of this kinetic model based on [4] to model catalytic recombination has been shown. At the current state of the art, experimental data on TPS catalyticity cannot yet be replaced with data calculated using models; however, the high cost of testing requires a careful preliminary screening of materials to test. This screening may be made easier models such as that used in this work.

Acknowledgement

The authors want to thank Daniele Gozzi in the Chemistry Department of the University of Rome "La Sapienza," Italy, for many useful discussions and for information on zirconia and the chemical bonds Zr–H and Zr–OH.

References

[1] Augelli, M., Bignami, G., Bruno, C., and Rubbia, C., "Report of the Working Group on a Preliminary Assessment of a New Fission Fragment Heated Propulsion Concept and its Applicability to Manned Missions to the Planet Mars" (Project 242), Agenzia Spaziale Italiana, Roma, March 1999.

[2] Buffone, C., and Bruno, C., "Nozzle Cooling in the Future Rubbia's Engine Test Facility," International Symposium on Space Technology and Science Paper 2002-c-1, 2002.

[3] Buffone, C., Bruno, C., and Sefiane, K., "Liquid Metal Heat Pipes for Cooling Rocket Nozzle Walls," AIAA Paper 2003-4452, July 2003.

[4] Barbato, M., Bruno, C., and Nasuti, F., "Material-Dependent Catalytic Recombination Modeling for Hypersonic Flows," *Journal of Thermophysics and Heat Transfer*, Vol. 10, No. 1, 1996, pp. 131–136.

[5] Atkins, P. W., and Beran, J. A., *General Chemistry*, 2nd ed., Scientific American Library, New York, 1992, pp. 320–325.

[6] Merle-Méjean, T., Barberis, P., Ben Othmane, S., Nardou, F., and Quintard, P. E., "Chemical Forms of Hydroxyls on/in Zirconia: An FT-IR Study," *Journal of the European Ceramic Society*, Vol. 18, No. 11, 1998, pp. 1579–1586.

[7] Trunschke, A., Hoang, D. L., and Lieske, H., "In Situ FTIR Studies of High-Temperature Adsorption of Hydrogen on Zirconia," *Journal of the Chemical Society Faraday Transactions*, Vol. 91, No. 24, 1995, pp. 4441–4444.

[8] Chase, M. W., Jr., "JANAF Thermochemical Tables," 3rd ed., *Journal of Physical and Chemical Reference Data*, Vol. 14, Supplement No. 1, 1985.

[9] Morse, P. M., "Diatomic Molecules According to the Wave Mechanics, Part 2: Vibrational Levels," *Physical Review*, Vol. 34, No. 1, July 1929, pp. 57–64.

[10] Gaydon, A. G., *Dissociation Energies*, Chapman and Hall, London, 1953, p. 30.

[11] Moelwyn-Huges, E. A., *Physical Chemistry*, 2nd ed., Pergamon Press, London, 1961, p. 407.

[12] Merle-Méjean, T., Barberis, P., Ben Othmane, S., Nardou, F., and Quintard, P. E., "Chemical Forms of Hydroxyls on/in Zirconia: An FT-IR Study," *Journal of the European Ceramic Society*, Vol. 18, No. 11, Oct. 1998, pp. 1579–1586.

[13] Jacob, K. H., Knözinger, E., and Benier, S., "Adsorption Sites on Polymorphic Zirconia," *Journal of Materials Chemistry*, Vol. 3, No. 6, 1993, pp. 651–657.

[14] Morterra, C., Cerrato, G., and Ferroni, L., "Surface Characterization of Yttria-Stabilized Tetragonal ZrO_2, Part 1: Structural, Morphological, and Surface Hydratation Features," *Materials Chemistry and Physics*, Vol. 37, No. 3, April 1994, pp. 243–257.

[15] Balasubramanian, K., and Wang, J. Z., "Spectroscopic Properties and Potential Energy Curves of Thirty-Six Electronic States of ZrH," *Chemical Physics Letters*, Vol. 154, Feb. 1989, pp. 525–530.

[16] Langhoff, S. R., Petterson, L. G. M., Bauschlicher, C. W., Jr., and Partridge, H., "Theoretical Spectroscopic Parameters for the Low-Lying States of the Second-Row Transition Metal Hydrides," *Journal of Chemical Physics*, Vol. 86, No. 1, 1987, pp. 268–278.

[17] Koseki, S., Ishihara, Y., Umeda, H., Fedorov, D. G., and Gordon, M. S., "Dissociation Potential Curves of Low-Lying States in Transition Metal Hydrides, Part 1: Hydrides of Group 4," *Journal of Physical Chemistry A*, Vol. 106, No. 5, 2002, pp. 785–794.

[18] Cacciatore, M., Rutigliano, M., and Billing, G. D., "Eley–Rideal and Langmuir-Hinshelwood Oxygen Atom Recombination Reaction on Silica: Energy Transfer and Recombination Coefficient Calculation," *Journal of Thermophysics and Heat Transfer*, Vol. 13, No. 2, 1999, pp. 195–203.

[19] Buffone, C., "Scambio di Calore in Ugelli Supersonici ad Alte Temperature," Master's Thesis, DMA, University of Rome "La Sapienza," 2000.

[20] Kratzer, P., and Breing, W., "Highly Excited Molecules from Eley–Rideal Reactions," *Surface Science*, Vol. 254, Aug. 1991, pp. 275–280.

[21] Barbato, M. C., "Heterogeneous Catalysis Model for Hypersonic Flight Simulations," ESA-ESTEC Document, YPA/1731/MB, Noordwijk, The Netherlands, pp. 35–36.

[22] Barbato, M., Reggiani, S., Bruno, C., and Muylaert, J., "Model for Heterogeneous Catalysis on Metal Surfaces with Application to Hypersonic Flows," *Journal of Thermophysics and Heat Transfer*, Vol. 14, No. 3, July–September 2000, pp. 412–420.

[23] Bruno, C., "Real Gas Effects," *Hypersonics*, edited by J. Periaux, J. J. Bertin, and R. Glowinski, Birkhäuser, Boston, 1989, pp. 303–354.

[24] Zoby, V., "Viscous Shock Layer Solutions with Nonequilibrium Chemistry for Hypersonic Flows Past Slender Bodies," *Research and Technology 1988, Annual Report of the NASA Langley Research Center*, NASA Rept. TM-4078, p. 107.

[25] Halpern, B., and Rosner, D. E., "Chemical Energy Accommodation at Catalyst Surfaces," *Journal of the Chemical Society Faraday Transactions 1*, Vol. 74, 1978, pp. 1883–1912.

[26] Masel, R. I., *Principles of Adsorption and Reaction on Solid Surfaces*, John Wiley and Sons, New York, 1996.

[27] Tully, J., "Dynamics of Gas-Surface Interactions: Reaction of Atomic Oxygen with Adsorbed Carbon on Platinum, *Journal of Chemical Physics*, Vol. 73, No. 12, Dec. 1980, pp. 6333–3642.

[28] Livage, J., Vivine, D., and Maziers, C., "Oxyde of Amorphous Zr Hydrate," *Reactivity of Solids: Proceedings of the 6th International Symposium on the Reactivity of Solids*, edited by J. W. Mitchell, Wiley–Interscience, New York, 1969.